

1 **Supplementary Material**

2 **Mammalian Ssu72 phosphatase preferentially considers tissue-specific actively**  
3 **transcribed gene expression by regulating RNA Pol II transcription**

4 (Running title: Tissue-specific plasticity regulated by Ssu72)

5

6 Hyun-Soo Kim<sup>1,□</sup>, Yoon Jeon<sup>2</sup>, Yoon Ok Jang<sup>3</sup>, Ho Lee<sup>2</sup>, Yong Shin<sup>3, □</sup>,

7 Chang-Woo Lee<sup>1,□</sup>

8

9 <sup>1</sup>Department of Molecular Cell Biology, Sungkyunkwan University School of Medicine,  
10 Suwon 16419, South Korea

11 <sup>2</sup>Graduate School of Cancer Science and Policy, Research Institute, National Cancer Center,  
12 Goyang 10408, South Korea

13 <sup>3</sup>Department of Biotechnology, College of Life Science and Biotechnology, Yonsei  
14 University, Seoul 03722, South Korea

15

16 □Corresponding authors: Yong Shin ([shinyongno1@yonsei.ac.kr](mailto:shinyongno1@yonsei.ac.kr); Tel.: +82-2-2123-2885);

17 Hyun-Soo Kim ([jazz7780@skku.edu](mailto:jazz7780@skku.edu); Tel.: +82-2-2123-2885); Chang-Woo Lee

18 ([cwlee1234@skku.edu](mailto:cwlee1234@skku.edu); Tel.: +82-31-299-6121)

19

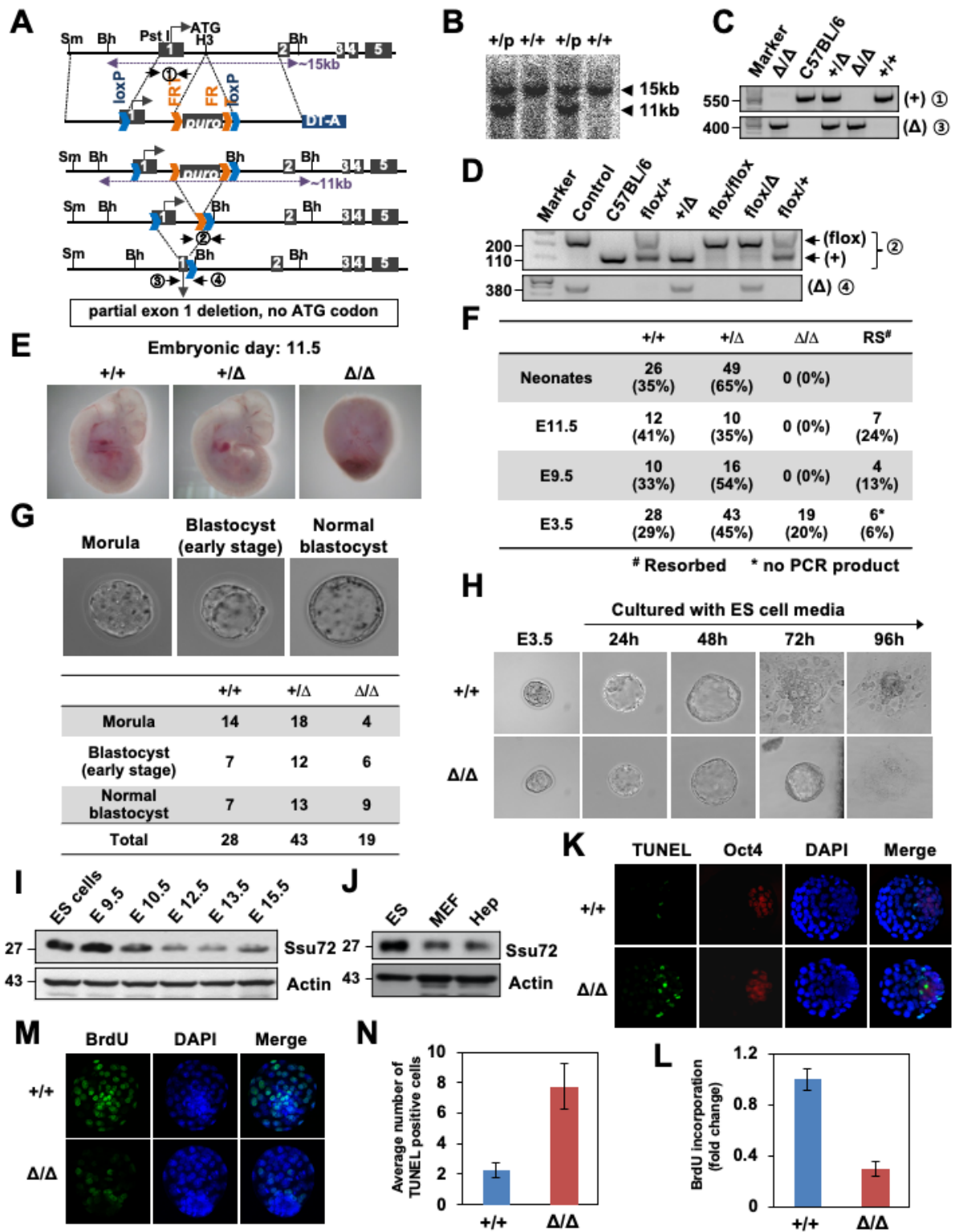
20

21

22

23

- 24 This file includes:
- 25 Figures S1 to S12
- 26 Supplementary methods



27

28

29

30 **Figure S1. Ssu72 loss causes developmental defects in mouse embryos.**

31 (A) Schematic representation of the Ssu72 locus, the targeting vector, and targeted,  
32 floxed, and deleted loci. Exon 1–5, translation start site (ATG), puromycin cassette  
33 (puro), diphtheria toxin A chain gene (DT-A), and restriction sites (Sm, *Sma*I; Bh,  
34 *Bam*HI; P, *Pst*I; H3, *Hind*III; Kp, *Kpn*I) are shown in the Ssu72 locus. The murine Ssu72  
35 gene located on chromosome 4E2 is composed of five exons with a potential  
36 translational start codon in exon 1 (NCBI annotation of NCBI Build 37.2). The targeting  
37 strategy was designed to flank Ssu72 exon 1 with *loxP* sites, allowing Cre-mediated  
38 exon 1 deletion. (B) Ssu72<sup>+/+</sup> and Ssu72<sup>+/p</sup> ES cell clones were subjected to Southern  
39 blot analyses. After *Bam*HI digestion, bands representing wild-type and mutant alleles  
40 are ~15 and ~11 kb, respectively. The symbol “p” represents the puromycin allele. (C)  
41 PCR analyses with genomic DNA extracted from mouse tails. The circled number  
42 represents a PCR reaction with primers described in Figure S1A. (D) PCR analyses  
43 with genomic DNA from mice containing floxed and deleted loci. The circled number  
44 represents a PCR reaction with primers described in Figure S1A. (E) Images of wild-  
45 type (<sup>+/+</sup>), heterozygous (<sup>+/ $\Delta$</sup> ), and homozygous ( <sup>$\Delta$ / $\Delta$</sup> ) mutant embryos at embryonic day  
46 11.5 (E11.5). Heterozygous Ssu72<sup>+/ $\Delta$</sup>  mice were seemingly normal, healthy, and fertile  
47 without developmental abnormalities during a 12-month or longer observation period.  
48 (F) Genotypes of progeny from Ssu72-heterozygous intercrosses by PCR analysis are  
49 shown. (G) Images of embryos at embryonic day 3.5 (E3.5). Those embryos were  
50 classified according to their appearance: morula, blastocyst (early stage), and normal  
51 blastocyst. Genotypes of embryos at E3.5 from Ssu72-heterozygous intercrosses are  
52 shown in the table. Genotyping analysis of 90 embryos from Ssu72<sup>+/ $\Delta$</sup>  mice  
53 intercrosses at embryonic days 3.5–4.5 (E3.5–4.5) revealed that 28 embryos were

54 wild-type ( $^{+/+}$ ), 43 embryos were  $^{+/\Delta}$ , and 19 embryos were  $^{\Delta/\Delta}$ . (H) Blastocyst stage  
55 embryos recovered at E3.5 were cultured *in vitro* for 24, 48, 72, and 96 h. (I)  
56 Expression levels of Ssu72 in indicated mouse ES cells during early embryogenesis.  
57 (J) Expression levels of Ssu72 in ES cells, MEFs, and hepatocytes. (K) Ssu72 $^{+/+}$  and  
58 Ssu72 $^{\Delta/\Delta}$  embryos were fixed and double-stained for TUNEL (green) and Alexa 546  
59 (Oct4; red). (L) Graph representing the average number of TUNEL-positive cells. Error  
60 bars indicate SD. (M) BrdU-incorporated Ssu72 $^{+/+}$  and Ssu72 $^{\Delta/\Delta}$  embryos were fixed  
61 and immunostained with anti-BrdU (green). (N) Graph representing values of relative  
62 BrdU incorporation. Error bars indicate SD.

63

64

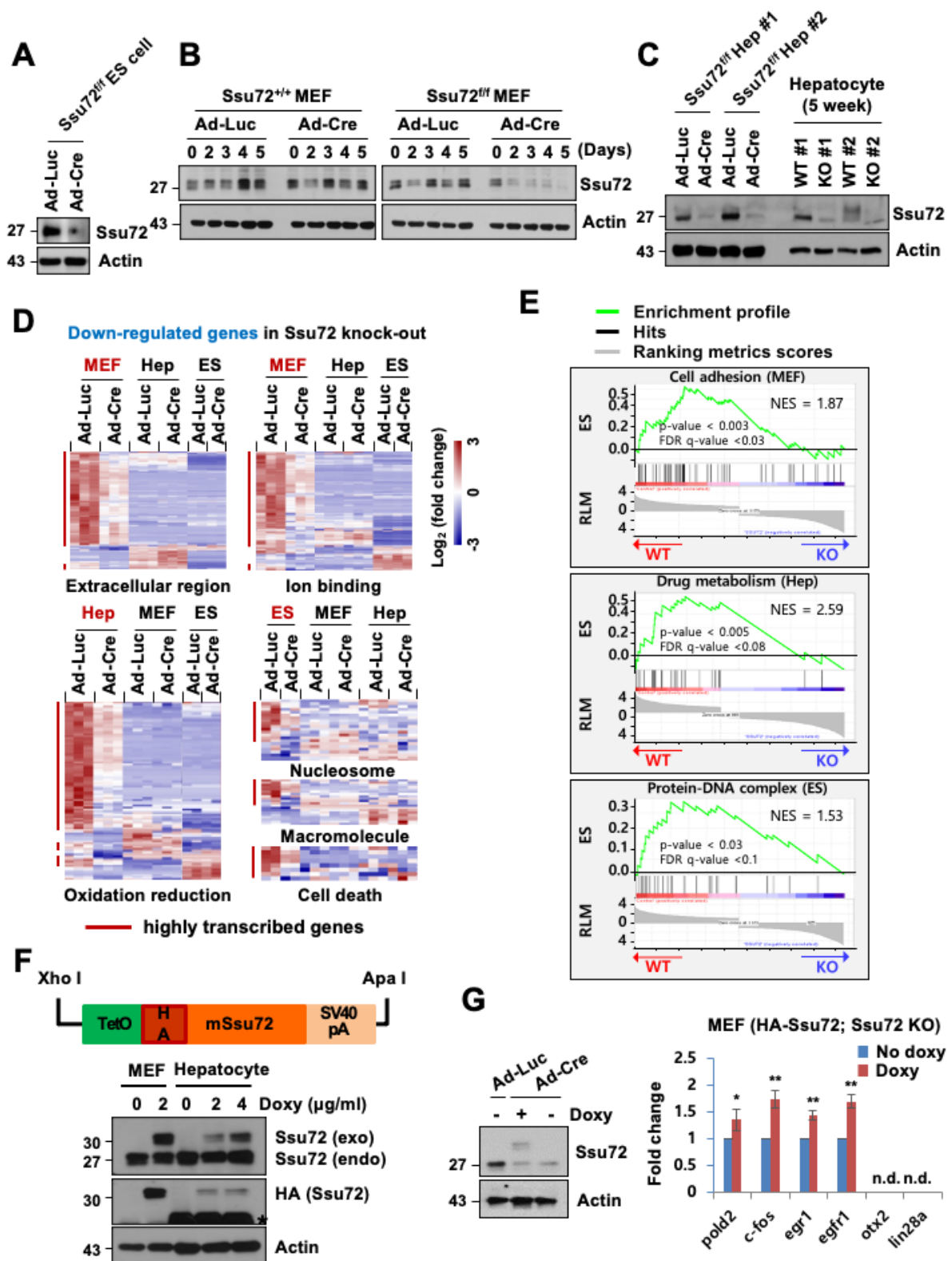
65

66

67

68

69



70

71

72

73 **Figure S2. Validations of Cre adenoviruses, RNA-Seq heatmap data, GSEA**  
74 **analyses, and HA-Ssu72 transgenic mice.**

75 (A) *Ssu72<sup>ff</sup>* ES cells were infected with Ad-Luc and Ad-Cre for 12 h and cultured for 3  
76 days with fresh media. ES cells were harvested and immunoblotted with anti-Ssu72  
77 and anti-actin antibodies. (B) *Ssu72<sup>+/+</sup>* and *Ssu72<sup>ff</sup>* MEFs were infected with Ad-Luc  
78 and Ad-Cre for 12 h. At the indicated time, MEF cells were harvested and  
79 immunoblotted with anti-Ssu72 and anti-actin antibodies. (C) Ad-Luc-infected or Ad-  
80 Cre-infected hepatocyte extracts were immunoblotted with antibodies indicated (left  
81 panels). Hepatocytes from *Ssu72<sup>ff</sup>* mice and Alb-Cre;*Ssu72<sup>ff</sup>* mice were harvested  
82 and immunoblotted with antibodies indicated (right panels). (D) Gene ontology-based  
83 heatmaps of down-regulated genes between control (Ad-Luc-infected) and *Ssu72*-  
84 depleted (Ad-Cre-infected) MEFs, hepatocytes, and ES cells. Subsets of genes down-  
85 regulated by *Ssu72* depletion in each cell type (red) are compared with different cell  
86 types (black). Red lines denote transcriptionally active genes in each cell type. The  
87 color bar represents the gradient of log<sub>2</sub>-fold changes for each cell type. (E) Gene set  
88 enrichment analysis (GSEA) enrichment plot of down-regulated gene sets in *Ssu72*-  
89 depleted MEFs, hepatocytes, and ES cells versus related gene sets (MEF: cell  
90 adhesion; Hep: drug metabolism; ES: protein–DNA complex). The green curve shows  
91 the enrichment score, reflecting the degree to which each gene was enriched (black  
92 vertical lines). (F) The vector construct used to generate doxycycline (Doxy)-inducible  
93 HA-tagged *Ssu72* transgenic mice. TetO (promoter containing tetracycline operator  
94 sequence), HA (hemagglutinin epitope tag), m*Ssu72* (mouse *Ssu72* sequence), and  
95 SV40pA (SV40 early polyadenylation signal) are shown. The vector was linearized,  
96 purified, and injected into the pronuclei of fertilized C57BL/6J mice. MEFs and

97 hepatocytes expressing HA-tagged Ssu72 were cultured in the absence (-) or  
98 presence (+) of Doxy. Cells were harvested and subsequently immunoblotted with  
99 indicated antibodies. (G) MEF extracts of Ssu72 WT, Ssu72 KO, and Ssu72 KO; HA-  
100 Ssu72 mice were immunoblotted with indicated antibodies. qPCR analyses of  
101 expression levels of various genes using Doxy-inducible HA-tagged Ssu72 transgenic  
102 MEFs under the Ssu72-depleted condition. Data are representatives of three  
103 independent experiments. Error bars indicate SD.

104

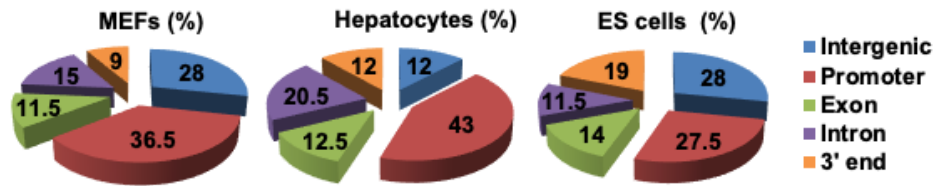
105

106

107

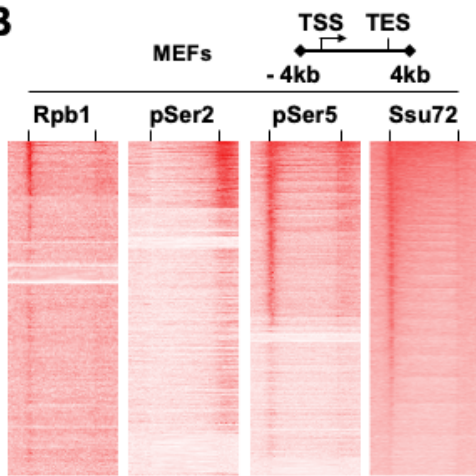


**A**

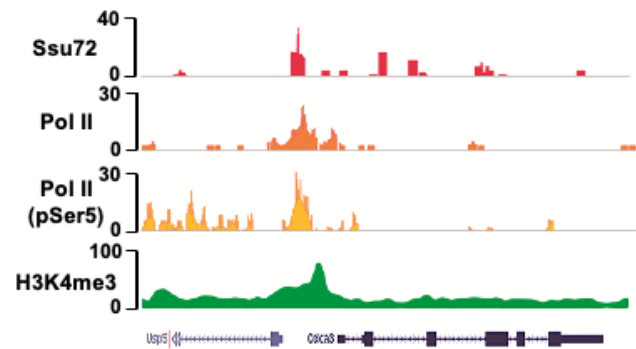


Distribution	MEFs_Ssu72 peaks	Hepatocytes_Ssu72 peaks	ES cells_Ssu72 peaks
Intergenic	1396	1349	1125
Promoter	1823	4835	1107
Exon	573	1404	563
Intron	748	2303	462
3' end	449	1346	763
Total	4989	11237	4020

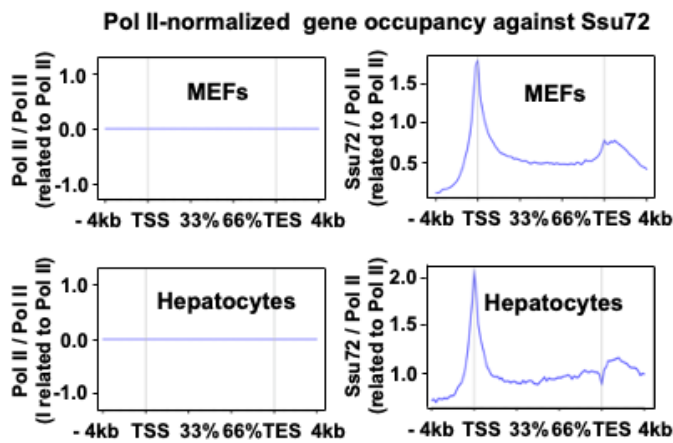
**B**



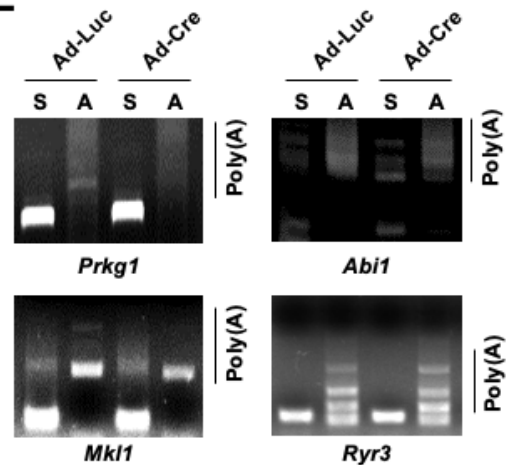
**C**



**D**



**E**



108

109

110

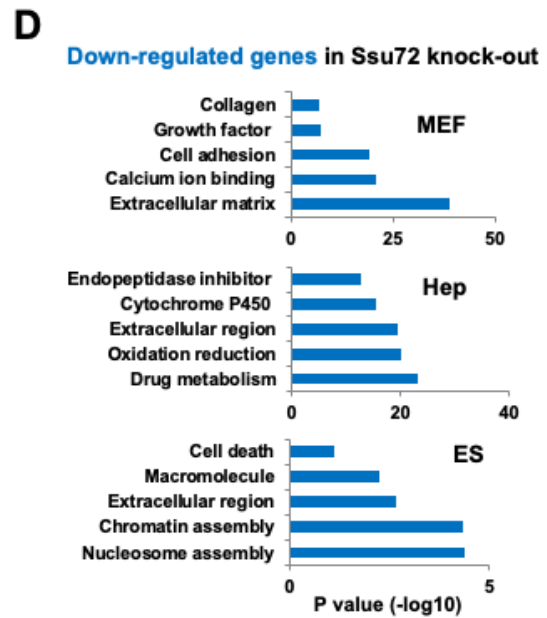
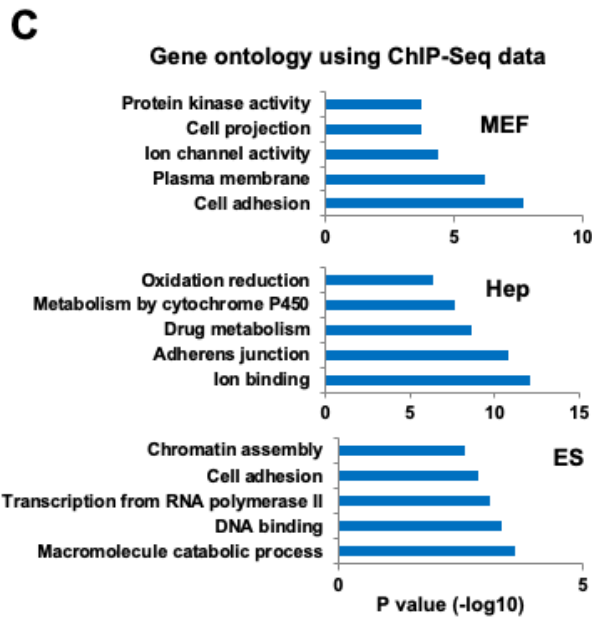
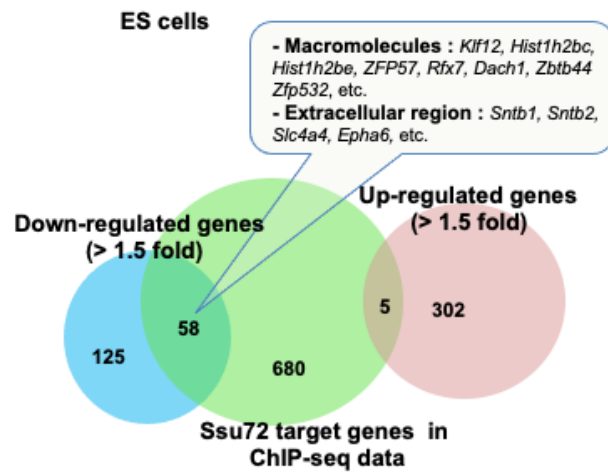
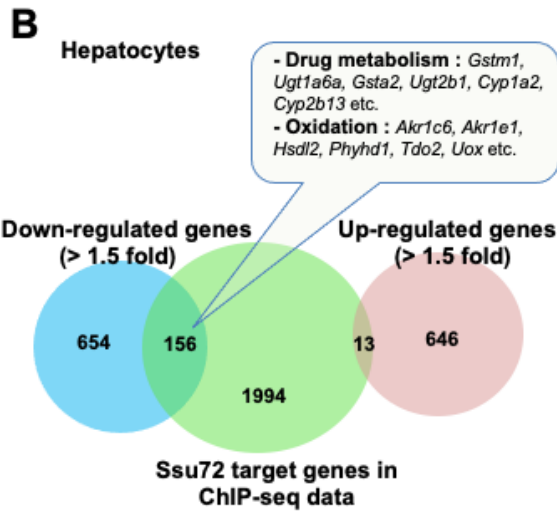
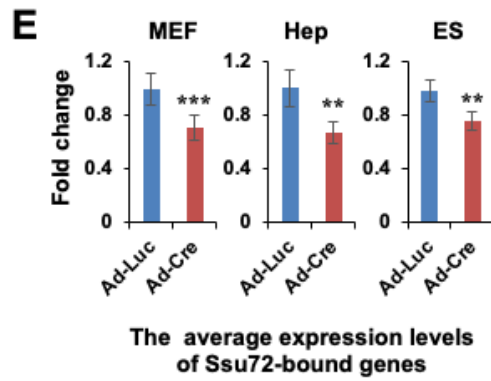
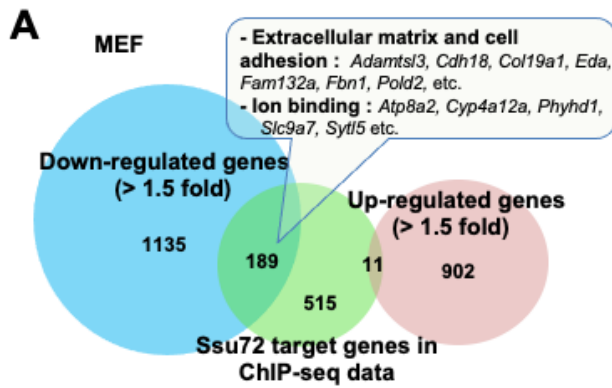
111

112 **Figure S3. Distribution of enriched Ssu72 ChIP-Seq signals.**

113 (A) Pie chart and table showing the genomic distribution of Ssu72 ChIP-Seq peaks  
114 with respect to various gene landmarks, including promoter (within  $\pm$  1 kb of TSS),  
115 exon, intron, 3'-end (within 4 kb downstream of the gene), and intergenic region in  
116 MEFs, hepatocytes, and ES cells. (B) Density plots of Rpb1 (first column), pSer2  
117 (second column), pSer5 (third column) and Ssu72 (fourth column) distributions at  
118 individual genes in MEFs. Each panel represents 4 kb upstream of TSS, the gene body,  
119 and 4 kb downstream of the TES. (C) ChIP-Seq signals for Ssu72, Pol II, pSer5, and  
120 H3K4me3 (GSE26657) across the indicated loci. (D) Pol II-normalized average gene  
121 occupancies of Ssu72 ChIP-Seq signals in MEFs and hepatocytes. (E) Comparison  
122 of mouse poly(A) tail-lengths in MEFs. S: gene specific PCR primer; A: Poly(A) tail  
123 PCR primer.

124

125



126

127

128

129 **Figure S4. The validation analyses by integrating Ssu72-related ChIP-Seq and**  
130 **RNA-Seq data**

131 (A and B) Venn diagram representing the overlap between the target genes against  
132 high-confidence Ssu72 ChIP-Seq peaks and the down- and up-regulated genes in  
133 Ssu72-depleted MEFs, hepatocytes and ES cells. (C) Gene ontology analyses of the  
134 Ssu72 target genes based on ChIP-Seq data of MEFs, hepatocytes, and ES cells. (D)  
135 Gene ontology analyses of the downregulated genes by Ssu72 depletion in MEFs,  
136 hepatocytes, and ES cells. (E) The average mRNA expression levels of the Ssu72-  
137 bound genes against high-confidence Ssu72 ChIP-Seq peaks in MEFs, hepatocytes,  
138 and ES cells based on RNA-Seq data. The asterisk denotes a difference according to  
139 Student's *t*-test (\*\*  $p < 0.01$ , \*\*\*  $p < 0.001$ ).

140

141

142

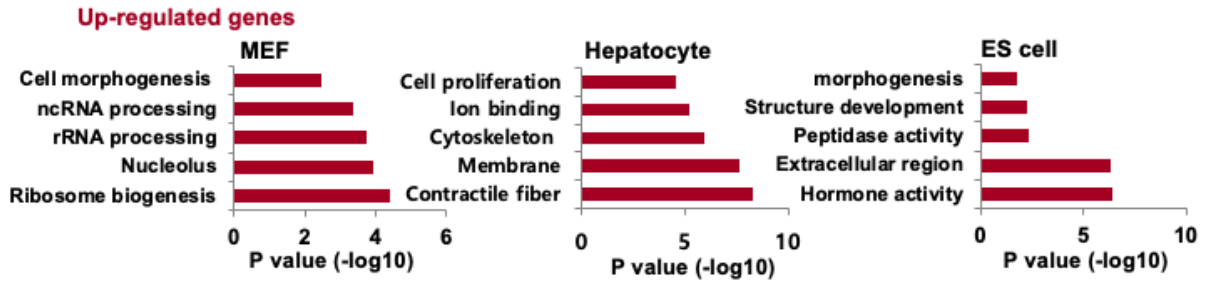
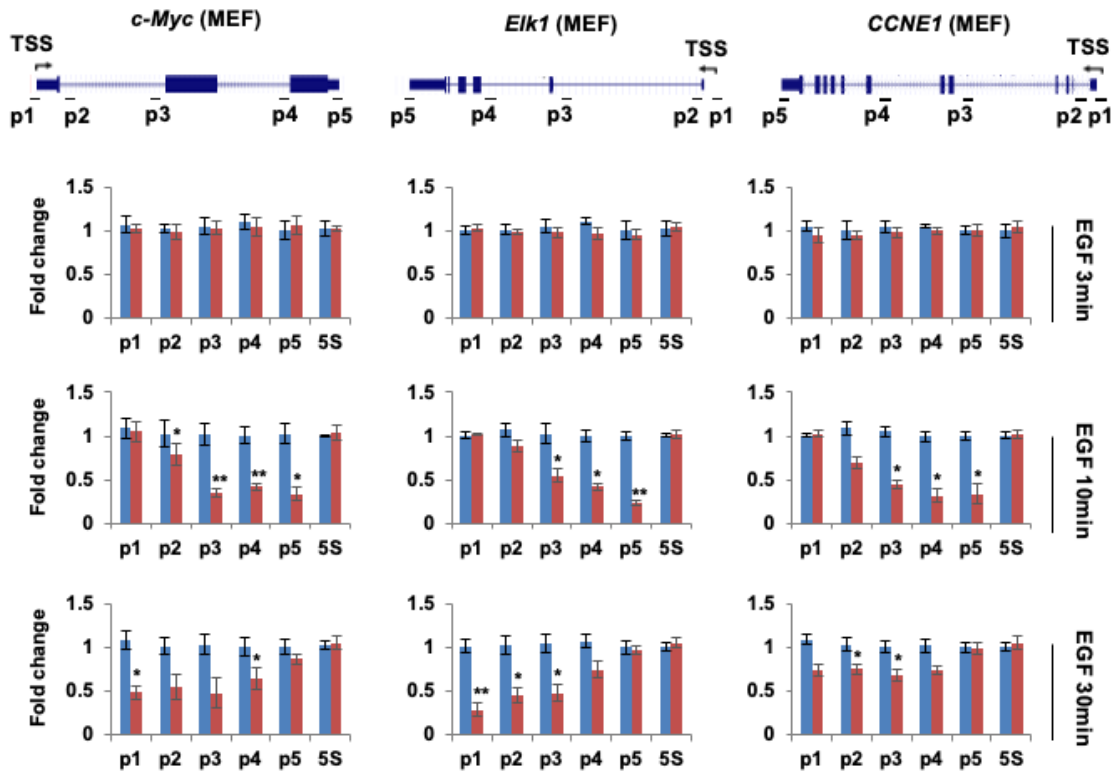
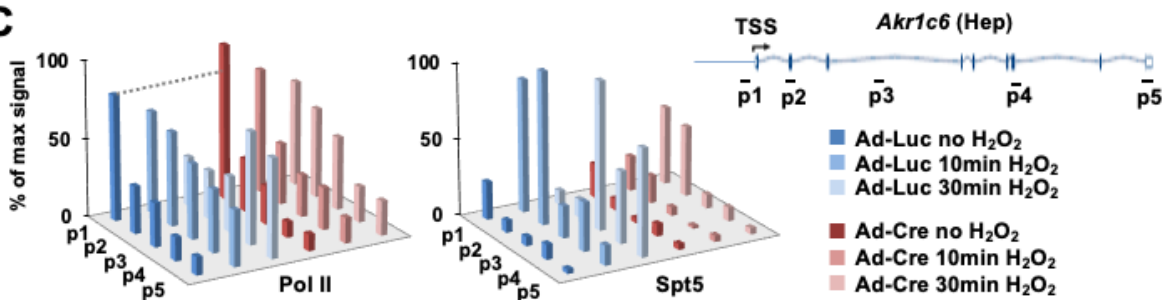
143

144

145

146

147

**A****B****C**

148

149

150

151

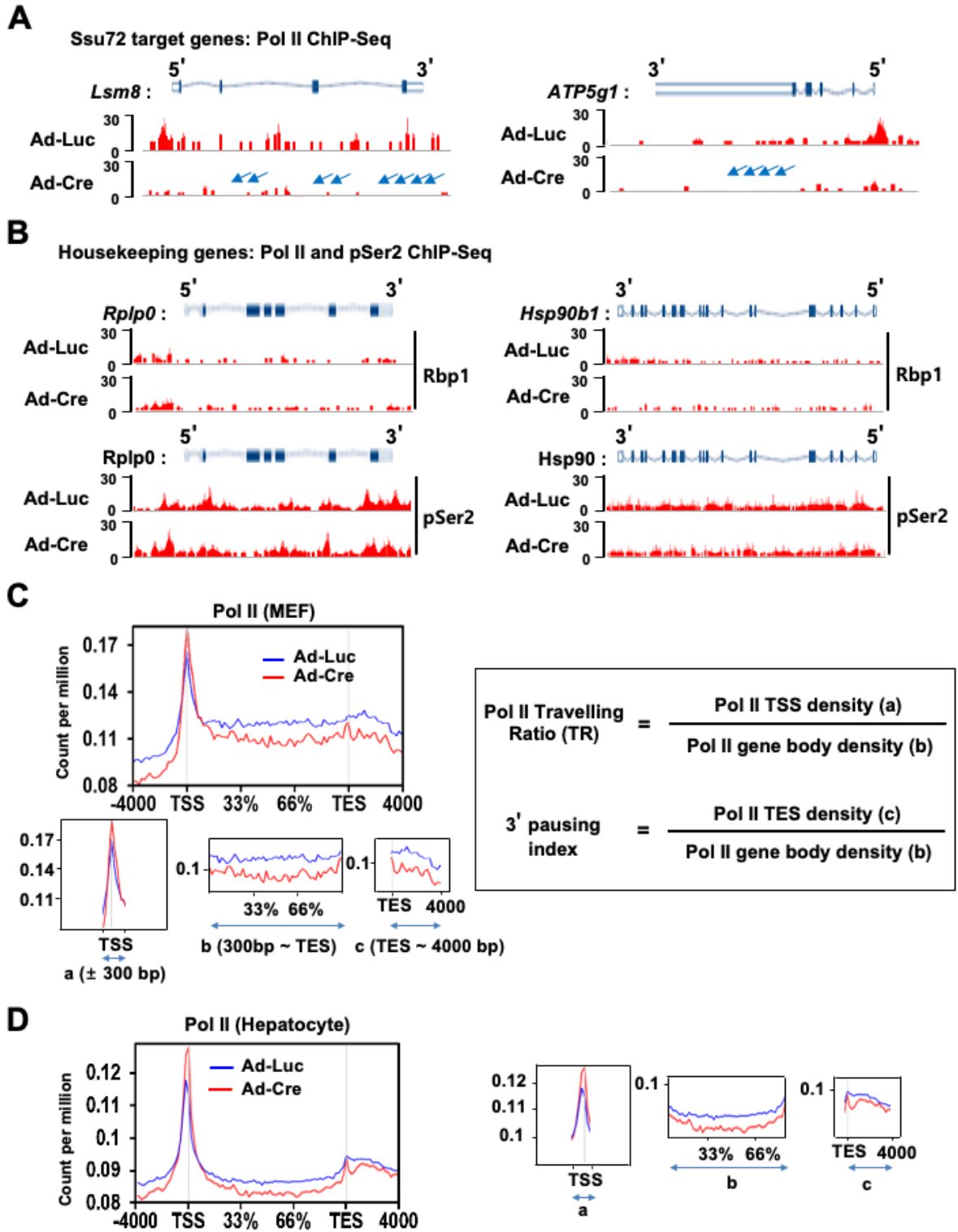
152 **Figure S5. The characterization of upregulated genes caused by Ssu72**  
153 **depletion, and ChIP analyses of Pol II and Spt5 in hepatocytes.**

154 (A) Gene ontology analyses of the upregulated genes by Ssu72 depletion in MEFs,  
155 hepatocytes, and ES cells. (B) Serum-deprived Ad-Luc or Ad-Cre-infected MEFs  
156 treated with EGF for the indicated time periods and analyzed by qRT-PCR using  
157 intronic primers (p1 ~ p6) of indicated gene. Error bars indicate SD. (C) ChIP and  
158 qPCR analyses of Pol II and Spt5 using primers (p1 ~ p5) of Akr1c6 gene in H<sub>2</sub>O<sub>2</sub>  
159 treated control and Ssu72-depleted hepatocytes. Prior to harvest, Ad-Luc or Ad-Cre-  
160 infected hepatocytes were stimulated with 100 μM H<sub>2</sub>O<sub>2</sub> for 10 and 30 min, respectively.  
161 A schematic representation of Akr1c6 gene and locations of primer sets for qPCR  
162 analysis are shown in the upper panel.

163

164

165



166

167

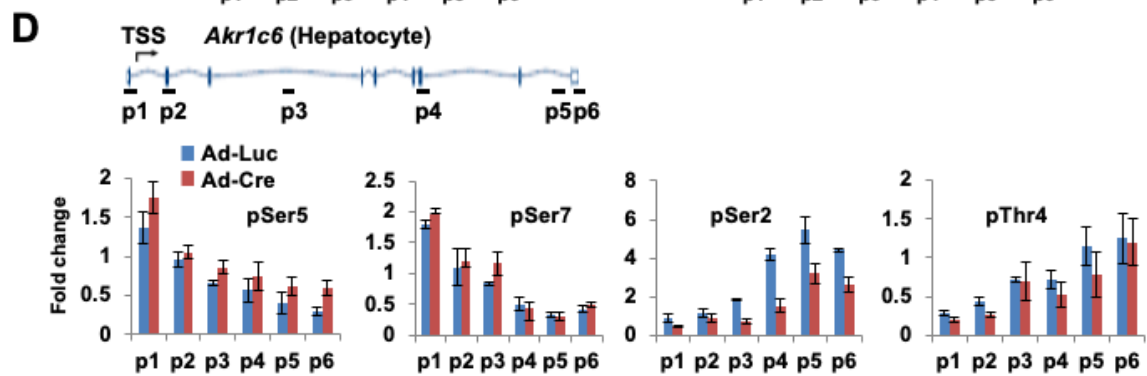
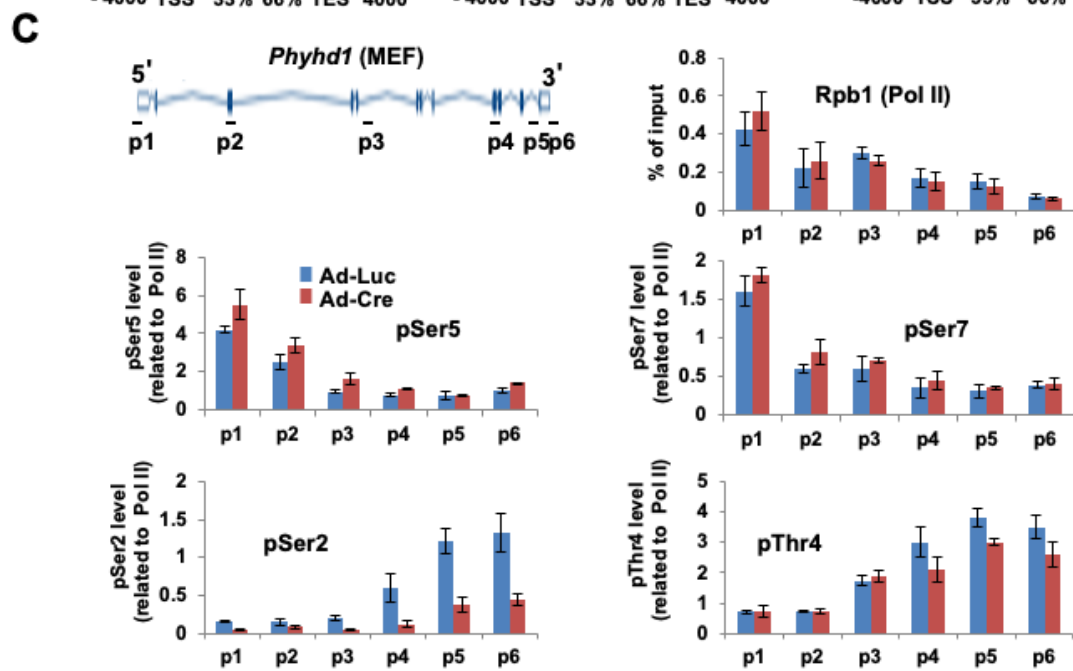
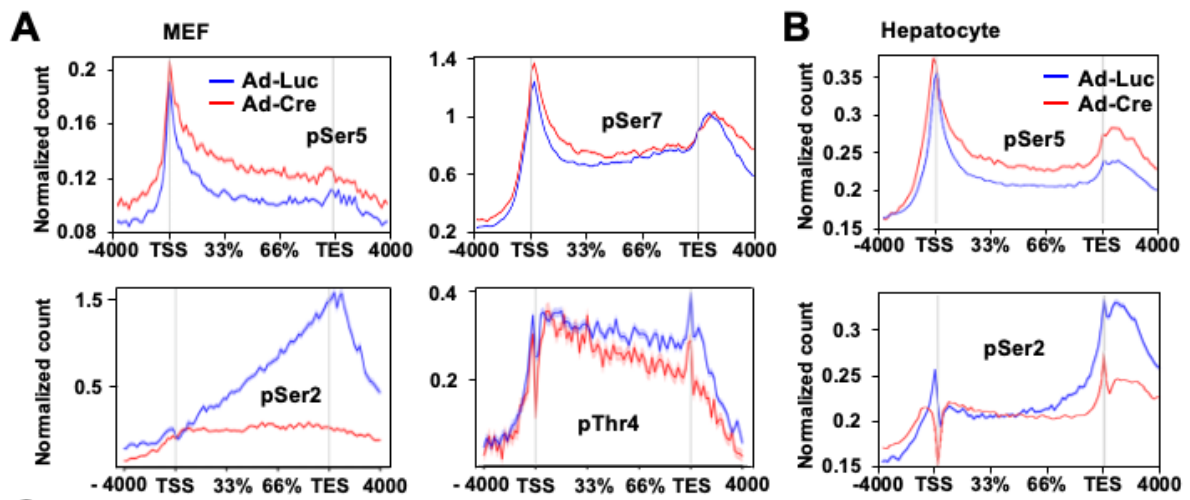
168

169 **Figure S6. Genome browser views of Ssu72 target genes and housekeeping**  
170 **genes and traveling ratio calculation.**

171 (A) Genome browser views of Pol II ChIP-Seq signals against various Ssu72 target  
172 genes in control and Ssu72-depleted MEFs. Schematic representation of several  
173 genes is shown at the top panel. Blue arrows indicate decreased Pol II signals in  
174 overall gene regions. (B) Genome browser views of Rpb1 (Pol II) and pSer2 ChIP-Seq  
175 signals against housekeeping genes (Rplp0 and Hsp90). (C) The genome-wide Pol II  
176 occupancy profiles describing the calculation used to determine the traveling ratio (TR)  
177 and 3' pausing index at each Pol II-bound gene in Ad-Luc and Ad-Cre infected MEFs.  
178 Promoter-proximal bin 'a' is defined using a fixed window from -300 to +300 bp around  
179 the annotated TSS. The gene body region 'b' bin is from + 300 bp to the annotated  
180 TES. The transcription termination region 'c' bin is from TES to + 4,000 bp after TES.  
181 TR is the ratio of Pol II density in the promoter-proximal 'a' bin to Pol II occupancy in  
182 the gene body region 'b' bin. The 3' pausing index is ratio of Pol II density in the  
183 termination region 'c' bin to Pol II occupancy in the gene body region 'b' bin. (D) The  
184 TR and 3' pausing index of Pol II occupancy profiles in Ad-Luc and Ad-Cre infected  
185 hepatocytes.

186





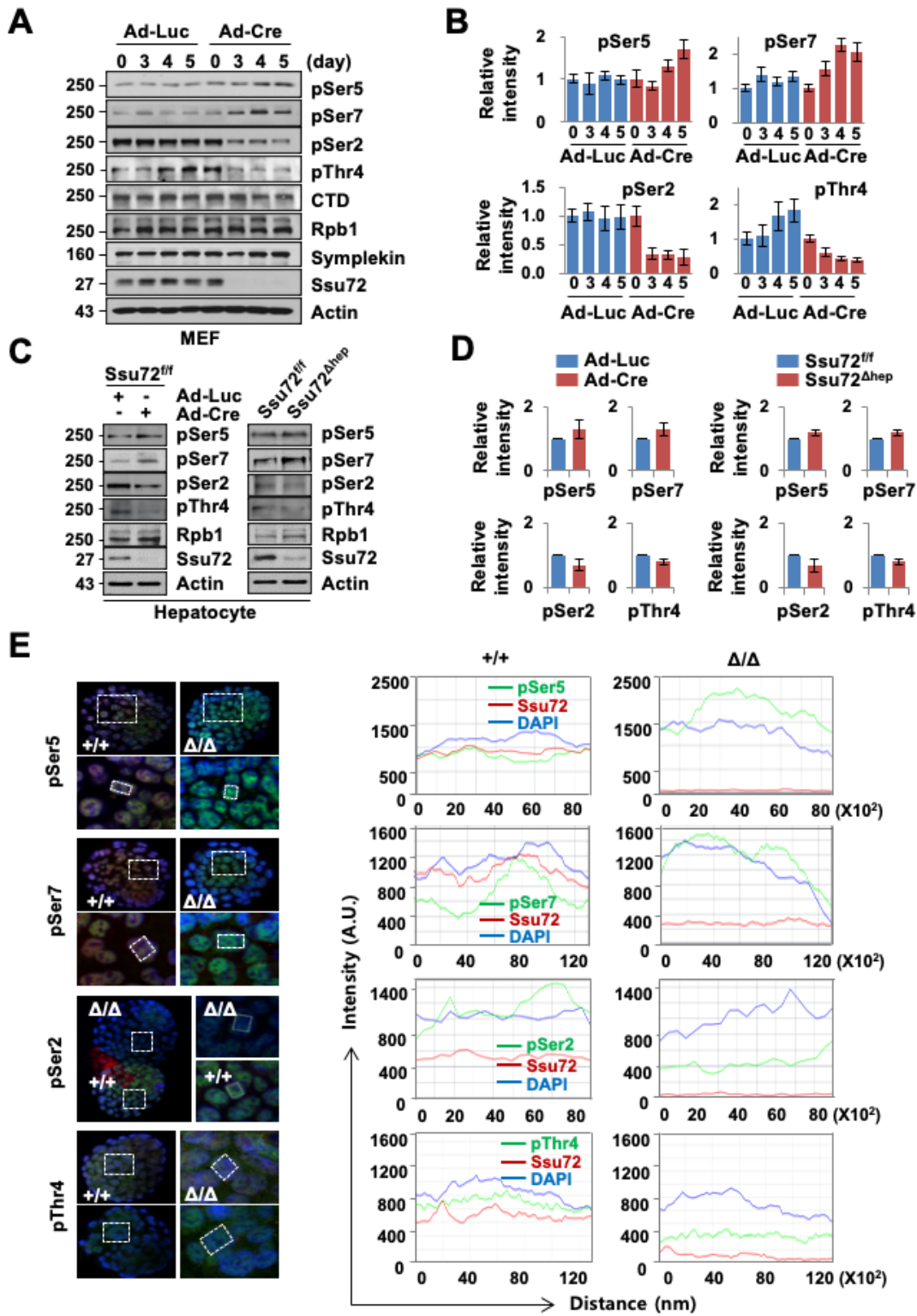
187

188

189

190 **Figure S7. Loss of Ssu72 results in abnormal phosphorylation of CTD code.**

191 (A) Pol II-normalized average gene occupancies of pSer5-, pSer2-, pSer7-, and pThr4-  
192 Pol II phosphorylation in control (Ad-Luc) and Ssu72-depleted (Ad-Cre) MEFs. (B) Pol  
193 II-normalized average gene occupancies of pSer5- and pSer2-Pol II phosphorylation  
194 in control (Ad-Luc) and Ssu72- depleted (Ad-Cre) hepatocytes. (C) ChIP and qPCR  
195 analyses of Pol II and Pol II-normalized pSer5, pSer7, pSer2, and pThr4 against  
196 Phyhd1 gene in control and Ssu72-depleted MEFs. Data are represented as mean  
197 value  $\pm$  SD of three independent experiments. (D) ChIP and qPCR analyses of pSer5,  
198 pSer7, pSer2, and pThr4 against Akr1c6 gene in control and Ssu72-depleted  
199 hepatocytes. Data are representatives of three independent experiments. Error bars  
200 indicate SD.



201

202

203

204 **Figure S8. Ssu72 is required for correct phosphorylation pattern of CTD in MEFs,**  
205 **hepatocytes and ES cells.**

206 (A) Ad-Luc or Ad-Cre-infected MEF cell extracts immunoblotted with indicated  
207 antibodies. (B) Quantified band intensity of phosphorylated CTD residues shown in  
208 Figure S8A with ImageJ software. Data are representatives of five independent  
209 experiments. (C) Extracts of Ad-Luc or Ad-Cre-infected and albumin-Cre cross-mated  
210 hepatocytes analyzed by immunoblotting with indicated antibodies. (D) Quantified  
211 band intensity of phosphorylated CTD residues shown in Figure S8C. (E) Fixed  
212 Ssu72<sup>+/+</sup> and Ssu72 $\Delta/\Delta$  embryos immunostained with anti-Ssu72 (Red) and various  
213 anti-phospho-CTD antibodies (Green; pSer5, pSer7, pSer2, and pThr4, respectively,  
214 Left panels). Representative single-cell traces (dotted square) of immunostained  
215 levels are quantified using ZEN 2012 blue edition software. Red, Ssu72; Green, pSer5,  
216 pSer7, pSer2, and pThr4; Blue, DAPI; Middle panels.

217

218

219

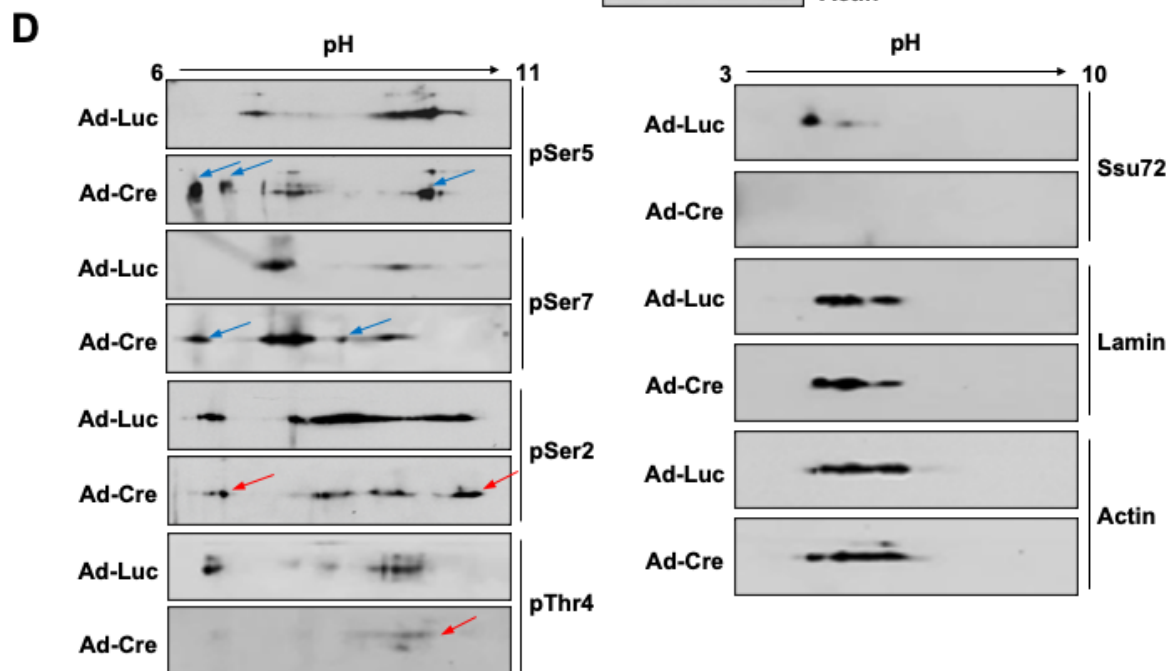
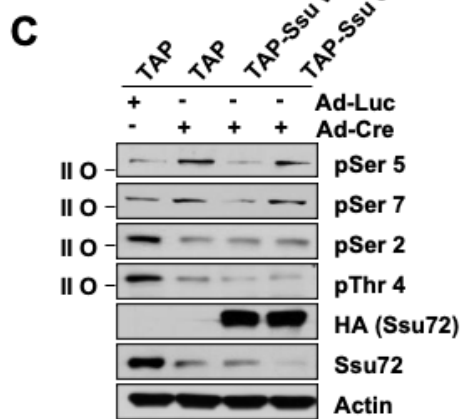
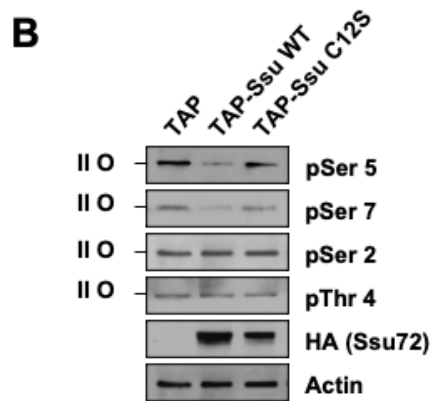
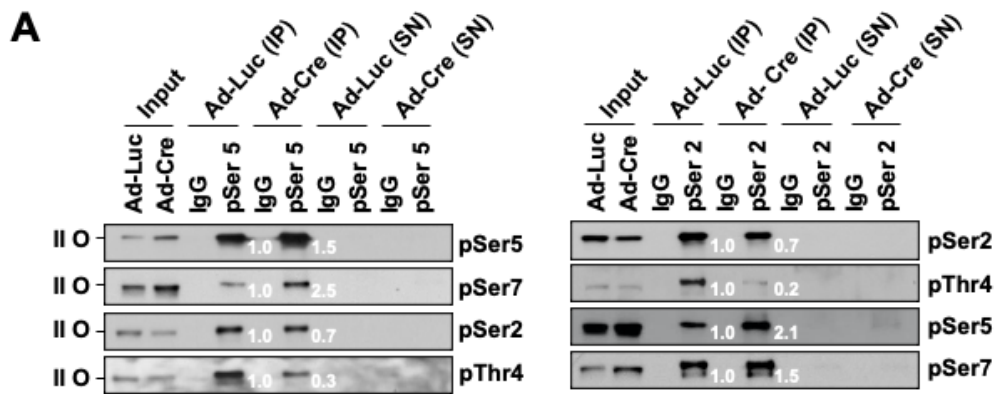
220

221

222

223

224



225

226

227

228 **Figure S9. The hyper-phosphorylation of Ser5 and Ser7 by Ssu72 depletion is**  
229 **directly coupled with the hypo-phosphorylation of Ser2 and Thr4**

230 (A) Ad-Luc or Ad-Cre-infected MEF cell extracts were immunoprecipitated with normal  
231 IgG, pSer5, or pSer2 antibodies, and then separated into two fractions, the immuno-  
232 complex pellets (IP) and soluble supernatants (SN). Respective IP and SN samples  
233 were analyzed by immunoblotting with phospho-specific antibodies against pSer2,  
234 pSer5, pSer7, and pThr4. The signal intensity of each phospho-polypeptide was  
235 quantified using Image J software. (B) *Ssu72<sup>ff</sup>* MEF cells were transfected with  
236 expression plasmids encoding TAP, TAP-Ssu72 WT, or TAP-Ssu72 C12S  
237 (phosphatase dead mutant). Cells were harvested and immunoblotted with the  
238 indicated antibodies. (C) *Ssu72<sup>ff</sup>* MEF cells were transfected with TAP, TAP-Ssu72 WT,  
239 or TAP-Ssu72 C12S expression plasmids, and then infected with Ad-Luc or Ad-Cre. At  
240 48 h post-transfection and further infection, cells were harvested and immunoblotted  
241 with the indicated antibodies. (D) Ad-Luc or Ad-Cre infected MEF cell extracts were  
242 analyzed by two-dimensional SDS-PAGE followed by immunoblotting with the  
243 indicated antibodies. Blue and red arrows indicate the acidic and basic shifts of  
244 phosphorylated CTD polypeptide spots, respectively.

245

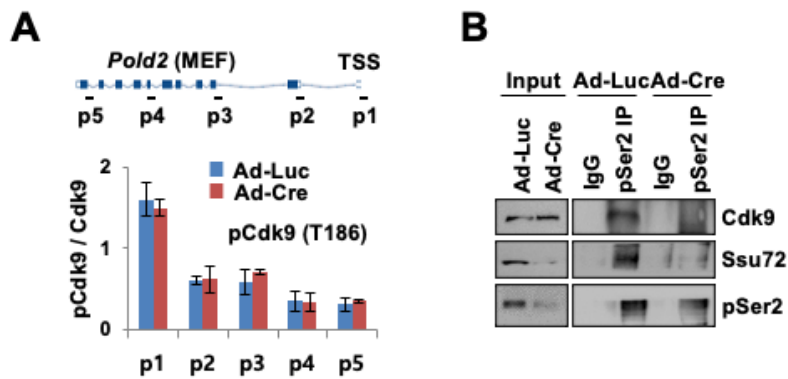
246

247

248

249

250

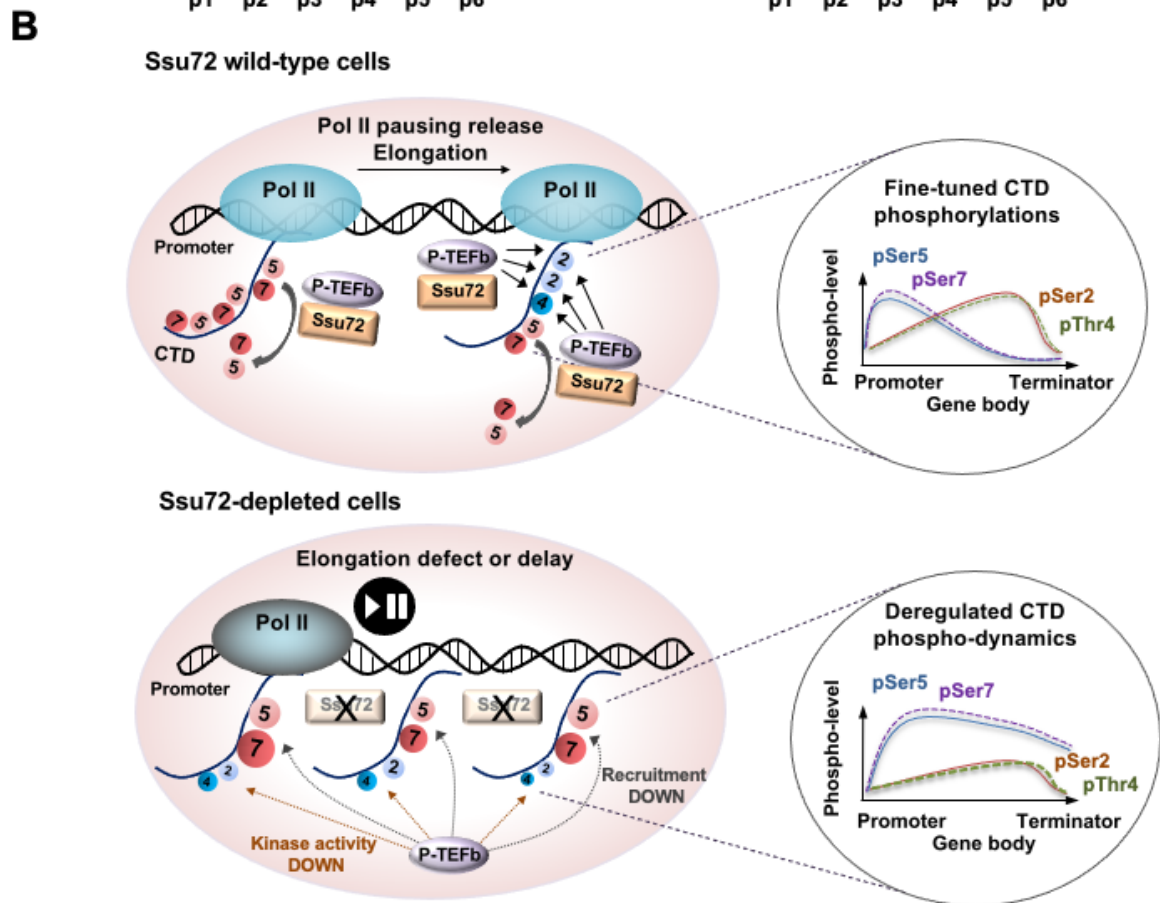
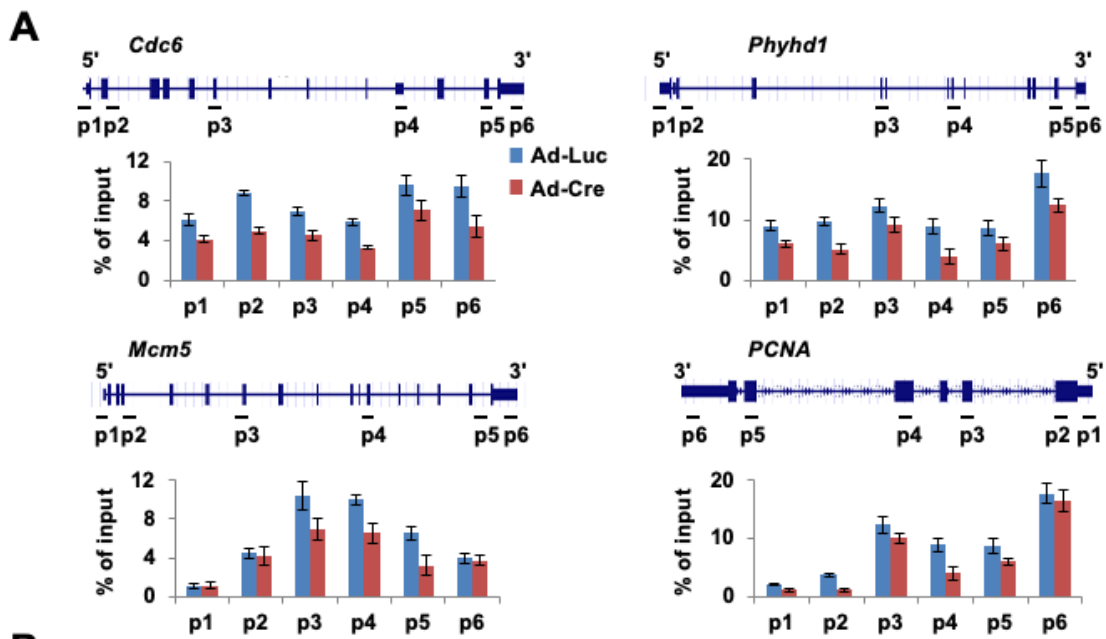


251

252 **Figure S10. The interaction analyses of Pol II and Pol II pSer2 under control and**  
 253 **Ssu72-depletion conditions**

254 (A) ChIP analyses of total Cdk9-normalized phospho-Cdk9 (T186) against *Pold2* gene  
 255 in control and Ssu72-depleted MEFs. (B) Extracts from Ad-Luc or Ad-Cre-infected  
 256 MEFs immunoprecipitated with IgG and anti-Pol II (pSer2) antibodies.  
 257 Immunocomplexes were analyzed by Western blotting using indicated antibodies.

258



259

260

261

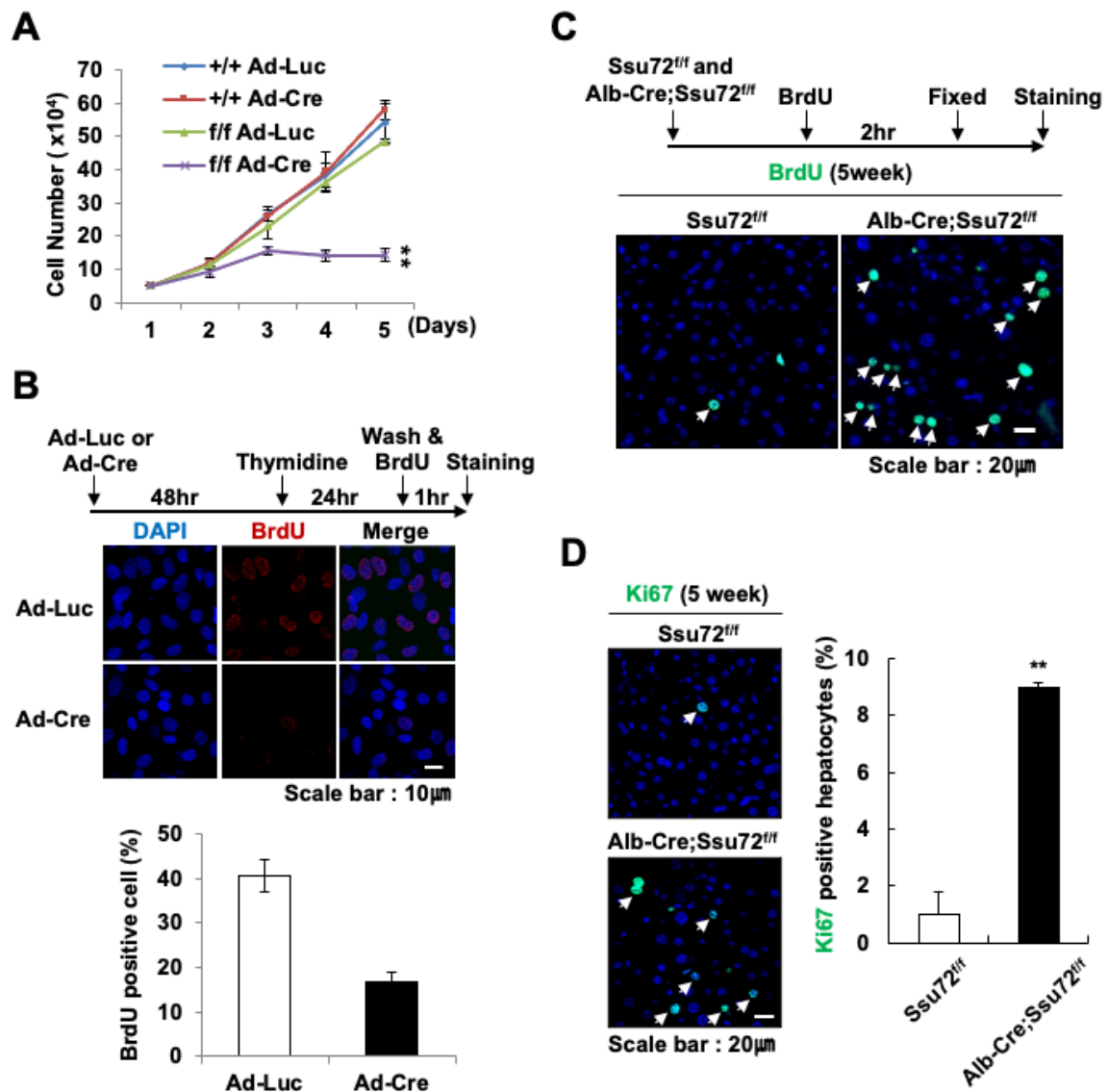


262 **Figure S11. The Cdk9 ChIP analyses and schematic model of transcriptional**  
263 **regulation by mammalian Ssu72**

264 (A) ChIP and qPCR analyses of Cdk9 against *Cdc6*, *Phyhd1*, *Mcm5* and *PCNA* genes  
265 in control and Ssu72-depleted MEFs. (B) Schematic model of transcriptional  
266 elongation activity and CTD phosphorylation profiles. See Results and Discussion  
267 sections for details.

268

269



270

271 **Figure S12. Ssu72 loss in mice results in distinct organ-specific phenotypes.**

272 (A) Growth plots of Ad-Luc or Ad-Cre infected Ssu72<sup>+/+</sup> and Ssu72<sup>ff</sup> MEFs by cell  
 273 number counting. Data are presented as mean value ± SD of three independent  
 274 experiments. The asterisk denotes a difference according to Student's t-test (\*\* p <  
 275 0.01). (B) Ssu72<sup>ff</sup> MEFs were infected with Ad-Luc or Ad-Cre, synchronized in G1/S  
 276 boundary by thymidine treatment, and released for 6 h. Cells were then incorporated  
 277 with BrdU for 1h. MEF cells were fixed and immunostained with anti-BrdU antibody

278 (upper panels). Scale bar represents 10  $\mu\text{m}$ . Quantification results of BrdU-positive  
279 signals in control and Ssu72 depleted MEFs are shown in the Bottom panel. Error bars  
280 represent SD from three independent experiments. (C) BrdU was administered to 5-  
281 week-old Ssu72<sup>ff</sup> and Alb-Cre; Ssu72<sup>ff</sup> mice by intraperitoneal injection (IP) 2 h before  
282 surgical extracting livers. Fixed liver sections were stained with anti-BrdU antibody.  
283 Arrows indicate BrdU-positive nuclei in hepatocytes. Scale bars represent 20  $\mu\text{m}$ . (D)  
284 Liver sections of 5-week-old Ssu72<sup>ff</sup> and Alb-Cre; Ssu72<sup>ff</sup> mice were stained with anti-  
285 Ki67 antibody (cell proliferation marker). Arrows indicate Ki67-positive nuclei in  
286 hepatocytes. Scale bars represent 20  $\mu\text{m}$ .

287

288

289

290

291

292

293

294

295

296

297

298

299 **Supplementary methods**

300 **In-gel digestion with trypsin and extraction of peptides**

301 Protein bands from SDS-PAGE gels were excised and in-gel digested with trypsin according  
302 to established procedures [1]. In brief, protein bands were excised from stained gels and cut  
303 into pieces. The gel pieces were washed for 1 h at room temperature in 25 mM ammonium  
304 bicarbonate buffer, pH 7.8, containing 50% (v/v) acetonitrile (ACN). Following the  
305 dehydration of gel pieces in a centrifugal vacuum concentrator (Biotron, Inc., Incheon, Korea)  
306 for 10 min, gel pieces were rehydrated in 50 ng of sequencing grade trypsin solution (Promega,  
307 Madison, WI, USA). After incubation in 25 mM ammonium bicarbonate buffer, pH 7.8, at 37 °C  
308 overnight, the tryptic peptides were extracted with 100 µL of 1 % formic acid (FA) containing  
309 50% (v/v) ACN for 20 min with mild sonication. The extracted solution was concentrated using  
310 a centrifugal vacuum concentrator. Prior to mass spectrometric analysis, the peptides solution  
311 was subjected to a desalting process using a reversed-phase column [2]. In brief, after an  
312 equilibration step with 10 ul of 5% (v/v) FA, the peptides solution was loaded on the column  
313 and washed with 10 ul of 5% (v/v) FA. The bound peptides were eluted with 8 ul of 70% ACN  
314 with 5% (v/v) formic acid.

315

316 **Identification of proteins by LC-MS/MS**

317 LC-MS/MS analysis was performed using a nanoACQUITY UPLC and LTQ-orbitrap-mass  
318 spectrometer (Thermo Electron, San Jose, CA, USA). For separation, a BEH C18 column (1.7  
319 µm, 100 µm × 100 mm; Waters, Milford, MA, USA) was used. The mobile phase for the LC  
320 separation was 0.1% FA in deionized water (A) and 0.1% FA in ACN (B). The chromatography  
321 gradient included a linear increase from 10% B to 40% B for 21 min, from 40% B to 95% B

322 for 7 min, and from 90% B to 10% B for 10 min. The flow rate was 0.5  $\mu$ L/min. For tandem  
323 mass spectrometry, mass spectra were acquired using data-dependent acquisition with full mass  
324 scan (300-2000  $m/z$ ), followed by MS/MS scans. Each MS/MS scan acquired was an average  
325 of one microscan on the LTQ. The temperature of the ion transfer tube was controlled at 275  $^{\circ}$ C,  
326 and the spray voltage was 2.0 kV. The normalized collision energy was set at 35% for MS/MS.  
327 The individual spectra from MS/MS were processed using the SEQUEST software (Thermo  
328 Quest, San Jose, CA, USA), and the generated peak lists were used to query the in-house  
329 database using the MASCOT program (Matrix Science Ltd., London, UK). We set the  
330 modifications of carbamidomethyl ('C'), deamidated ('NQ'), and oxidation ('M') for MS  
331 analysis and the tolerance of peptide mass was 10 ppm. The MS/MS ion mass tolerance was  
332 0.8 Da, the allowance of missed cleavage was 2, and charge states (+2, +3) were taken into  
333 account for data analysis. We took only significant hits, as defined by the MASCOT probability  
334 analysis.

335

### 336 **Two-dimensional SDS-PAGE**

337 For the first dimension, isoelectric focusing (IEF) was performed using the IPGphor system on  
338 pH 6-11 linear gradient IPG strips (Bio-Rad). Protein (200  $\mu$ g) was used for each two-  
339 dimensional gel. Samples were mixed with 200  $\mu$ l of rehydration buffer [8 M urea, 2% CHAPS,  
340 0.01% bromophenol blue, 1.2% Destreak reagent (GE Healthcare)] and 0.5% IPG buffer, and  
341 loaded in the IPGphor strip holder. The strips were then focused by the following program:  
342 rehydration for 10 h (no voltage); 0-500 V for 4 h; 500-1,000 V for 1 h; 1,000-8,000 V for 4 h;  
343 8,000 V for 20 min; and the final phase of 500 V from 20,000-30,000 Vh. After IEF, the IPG  
344 strips were first equilibrated in equilibration buffer 1 (6 M urea, 0.5 M Tris-HCl, pH 8.8, 30%  
345 glycerol, 2% SDS, 2% 2-mercaptoethanol) for 15 min, and further in equilibration buffer 2 (6

346 M urea, 0.5 M Tris-HCl, pH 8.8, 30% glycerol, 2% SDS, 2.5% iodoacetamide) for 15 min. The  
347 IPG strips were transferred onto the SDS-PAGE gels and performed the immunoblotting  
348 analyses.

349

350

351

## 352 **References**

353 1. Bahk YY, Kim SA, Kim JS, Euh HJ, Bai GH, Cho SN, et al. Antigens secreted from  
354 *Mycobacterium tuberculosis*: identification by proteomics approach and test for  
355 diagnostic marker. *Proteomics*. 2004; 4: 3299–307.

356 2. Gobom J, Nordhoff E, Mirgorodskaya E, Ekman R, Roepstorff P. Sample purification  
357 and preparation technique based on nano-scale reversed-phase columns for the sensitive  
358 analysis of complex peptide mixtures by matrix-assisted laser desorption/ionization mass  
359 spectrometry. *J Mass Spectrom*. 1999; 34: 105–16.

360